Magneto−Structural Correlation Studies of A Ferromagnetically Coupled Dinuclear Vanadium(IV) Complex. Single-Crystal EPR Study

Murugesan Velayutham, Babu Varghese, and Sankaran Subramanian*,†

Regional Sophisticated Instrumentation Centre, Indian Institute of Technology, Madras, Chennai-600 036, India

Received June 17, 1997

The dimer potassium dioxo(citrato)vanadate(IV)−6-water, $K_4\{VO[O_2CCH_2C(O)(CO_2)CH_2CO_2]\}_2 \cdot 6H_2O$, was prepared by the reaction of citric acid and metavanadate in a neutral solution. The complex crystallizes in the space group $P\bar{1}$ with unit cell parameters $a = 8.474(5)$ Å, $b = 8.902(7)$ Å, $c = 9.596(9)$ Å, $\alpha = 71.50(6)°$, $\beta = 70.81(9)°$, $\gamma = 87.45(2)°$, $V = 647.1$ Å^3, and $Z = 1$. The dimeric anion contains a centrosymmetric planar four-membered V_2O_2 ring with the bridging oxygens derived from the hydroxyl groups. The configuration of the anion is *anti-coplanar*. A frozen solution EPR spectrum with zero-field splitting and 15 line hyperfine patterns on the parallel and perpendicular features characteristic of two equivalent vanadium atoms confirms the presence of a spin triplet. This is further supported by the presence of half-field "forbidden transition" at $g \approx 4$. A broad line with half-field forbidden transitions in the powder EPR spectra at X,Q-bands of the neat sample and at different temperatures shows the presence of a spin triplet ground state and a very weak intermolecular dipolar interaction. From anisotropic exchange contributions to D the magnitude of the derived exchange integral J_{xy,x^2-y^2} is 56 cm^{-1}. UV−visible, ESCA, and theoretical BVS studies support the proposed molecular and electronic structure of the complex.

Introduction

The first biologically important role assigned to vanadium was as an inhibitor of Na^+, K^+-ATPases and nucleases.[1] Vanadium is present in all mammalian tissues at concentration of about 10 μM or less. Vanadium plays a significant role in the reduction of N_2 to NH_3.[2]

Citric acid is an important compound in biological processes. For example, citrates appear at about 0.1 mM in blood plasma and occur at 0.3 wt % in teeth and bone. They regulate some fundamental physiological processes and are intermediates in carbohydrate metabolism, e.g., in the "Krebs cycle".[3] Vanadium complexes are used as restriction enzymes to break the simple nucleotides and their polymers, *i.e.* DNA and RNA, and also used as anticancer drugs.[4] A recent work has focused on the insulin-mimicking properties of vanadium compounds.[5−7] The anionic complexes of VO^{2+} ion with α-hydroxy carboxylate anions in which both hydroxyl and carboxyl protons are removed exhibit novel structural, optical, and magnetic properties. Citric acid, acting as a tetradentate ligand, readily forms polynuclear complexes with numerous metal ions.[8] Citric acid under different experimental conditions directs the metal atoms to different oxidation states.[9]

A more detailed understanding of the nature of vanadium and biologically important ligands such as citric acid interactions necessitates a detailed knowledge of the coordination environment and oxidation state of the metal(s) within the systems. The study of magnetic properties of molecular compounds is of relevance for the understanding of magnetically coupled active sites in metalloproteins as well as their potential applications as magnetic materials. Most dimeric oxovanadium(IV) complexes exhibit an antiferromagnetic exchange interaction while a few complexes are reported to yield a ferromagnetic interaction.[10] By studying the molecular, electronic structures, and magnetic properties using different instrumental techniques, it is possible to design ligand environments to introduce specific magnetic properties to dinuclear d^1-d^1 systems containing two oxovanadium centers. We report in this paper the synthesis, molecular and electronic structures, magnetic properties, and physicochemical properties of the complex $K_4[VO(cit)]_2 \cdot 6H_2O$ (cit = citrate ion).

Experimental Section

Preparation of $K_4[VO(cit)]_2 \cdot 6H_2O$. Ammonium metavanadate (10 mmol) and an excess of citric acid (15 mmol) were dissolved in water, and the solution was refluxed for 0.5 h, adjusted to neutral pH by 10% potassium hydroxide, and stirred for several hours. The dark blue mixture was filtered and evaporated, and the solid formed was colletced and recrystallized to give a blue solid.

Physical Measurements. UV/vis spectra were recorded on an Shimadzu UV-3100 spectrometer. All the EPR spectra were recorded with a Varian E112 spectrometer (X- and Q-band frequencies) at 77

† Present address: Radiation Biology Branch, National Cancer Institute, National Institutes of Health, Bethesda, MD 20892. E-mail: subu@helix.nih.gov. Fax: (301) 480 2238.

(1) Cantley, L. C.; Josephson, L.; Warner, R.; Yanagisawa, M.; Lechene, C.; Guidotti, G. *J. Biol. Chem.* **1977**, *252*, 7421.
(2) Rehder, D. *Angew. Chem., Int. Ed. Engl.* **1991**, *30*, 148.
(3) Djordjevic, C.; Lee, M.; Sinn, E. *Inorg. Chem.* **1989**, *28*, 719.
(4) Dean, N. S.; Mokry, M.; Bond, M. R.; O'Conor, C. J.; Carrano, C. J. *Inorg. Chem.* **1996**, *35*, 2818.
(5) Codd, R.; Hamblay, T. W.; Lay, P. A. *Inorg. Chem.* **1995**, *34*, 877.
(6) Sun, Y.; James, B. R.; Rettig, S. J.; Orvig, C. *Inorg. Chem.* **1996**, *35*, 1667.
(7) Hanson, G. R.; Sun, Y.; Orvig, C. *Inorg. Chem.* **1996**, *35*, 6507.
(8) Kiss, T.; Buglyo, P.; Sanna, D.; Micera, G.; Decock, P.; Dewaele, D. *Inorg. Chim. Acta* **1995**, *239*, 145.
(9) Wright, D. W.; Humiston, P. A.; Orme-Johnson, W. H.; Davis, W. M. *Inorg. Chem.* **1995**, *34*, 4194.
(10) Plass, W. *Angew. Chem., Int. Ed. Engl.* **1996**, *35*, 627.

S0020-1669(97)00746-5 CCC: $15.00
Published on Web 03/06/1998

Table 1. Crystal and Structure Refinement Data of $K_4[VO(cit)]_2 \cdot 6H_2O$

empirical formula	$C_{12}H_{20}K_4O_{22}V_2$
fw	774.56
temp	293(2) K
wavelength	1.54184 Å
space group	$P\bar{1}$ (No. 2)
unit cell dimens	$a = 8.474(5)$ Å, $\alpha = 71.51(7)°$ $b = 8.903(8)$ Å, $\beta = 70.82(5)°$ $c = 9.597(6)$ Å, $\gamma = 87.45(7)°$
vol	647.1(8) Å^3
Z	1
D(calcd)	1.988 g cm^{-3}
abs coeff	120.76 cm^{-1}
$R(F_o)^a$	0.0530
$R_w(F_o^2)^a$	0.1503

[a] $R(F_o) = [\sum||F_o| - |F_c||/\sum F_o]$. $R_w(F_o^2) = \{\sum[w(F_o^2 - F_c^2)]^2/\sum[w(F_o)^2]^2\}^{1/2}$, where $w = 1/[\sigma(F_o^2)^2 + (0.1130P)^2 + (1.419P)]$ and $P = [\max(F_o^2,0) + 2F_c^2]/3$.

and 300 K. Variable-temperature (20−293 K) EPR was recorded using a CTI-Cryogenics set up. ESCA measurements were carried out using a VG Escalab MK II spectrometer under a vacuum of 10^{-9}−10^{-10} Torr. Bond valence sum analyses were also carried out for the complex.

X-ray Crystallography. A crystal of 0.3 mm × 0.3 mm × 0.2 mm size was mounted at the tip of a glass fiber attached to an Enraf-Nonius CAD4 diffractometer with Cu Kα radiation. A total of 25 reflections with $40° < 2\theta < 60°$ were collected through a random search routine and indexed using the principle of shortest vectors followed by least-squares refinement. A total of 2306 reflections with $2° < \theta < 70°$ were collected, with the $\omega-2\theta$ scan mode adopted for data collection, of which 2086 reflections had intensities with $I > 2\sigma(I)$. Two reflections whose intensities were monitored once every 1 h showed no decay of crystal during data collection. The data were corrected for Lorentz and polarization effects. The absorption correction was effected using ψ scan data. The structure was solved by direct methods using the SHELX-86 computer program and refined using SHELXL-93. All non-hydrogen atoms were refined with anisotopic thermal parameters. Hydrogen atoms were geometrically fixed, and a riding model refinement was effected. The final difference Fourier map showed 1.169 e/Å^3 as the highest peak. The final residual factors are $R(F_o) = 0.053$ and w$R(I) = 0.15$. The quantity minimized for least-squares refinement is $\sum w(F_o^2 - F_c^2)^2$, where $w = 1/[\sigma(F_o^2)^2 + (0.1130P)^2 + (1.419P)]$ and $P = [\max(F_o^2,0) + 2F_c^2]/3$. Table 1 presents the crystal and structure refinement data in brief.

Results and Discussion

Description of the Structure. The crystals separated from the products of the reaction between metavanadate and citric acid have 1:1 V:citrate mole ratio. Figure 1 shows the molecular structure of the complex. The complex crystallizes in the space group $P\bar{1}$ with one molecule per asymmetric unit. The crystal structure comprises discrete potassium cations, water molecules, and centrosymmetric dimeric anions. Selected bond lengths and bond angles are given in the Table 2. The presence of two coordinated bridging citrate ions makes the coordination polyhedron distort significantly from octahedral and also makes the V---V distance one of the shortest for dinuclear vanadyl complexes.[11] The chelation of the deprotonated hydroxy and carboxylic groups of the citrate ion leads to the presence of two six-membered rings and one five-membered ring, perhaps stabilizing the overall dimer moiety.

The core $[VO(\mu_2\text{-}O)]_2$ forms a centrosymmetric planar structure. The two vanadium atoms are in the basal plane, and the two citrate ions are sitting above and below the plane. The two vanadium−oxygen bond lengths involving the bridging

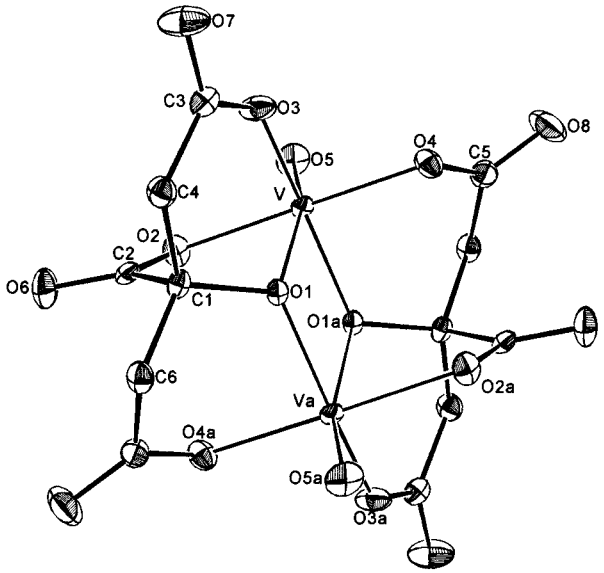

Figure 1. Molecular structure of $K_4[VO(cit)]_2 \cdot 6H_2O$. (ORTEP representation of the molecule depicting 50% propability ellipsoids.)

Table 2. Selected Bond Lengths (Å) and Bond Angles (deg) for $K_4[VO(cit)]2 \cdot 6H_2O^a$

V−O(1)	2.171(3)	V−O(1)#1	1.977(3)
V−O(2)	2.041(3)	V−O(3)	1.992(3)
V−O(4)	2.022(3)	V−O(5)	1.608(3)
V−V#1	3.301(3)	V−O(1)−V#1	105.39(13)
O(4)−V−O(1)	100.30(13)	O(1)#1−V−O(4)	87.91(13)
O(3)−V−O(4)	87.55(14)	O(5)−V−O(4)	95.8(2)
O(1)#1−V−O(1)	74.60(13)	O(3)−V−O(1)	80.89(12)
O(5)−V−O(3)	100.6(2)	O(5)−V−O(1)#1	105.5(2)
O(2)−V−O(1)	75.78(12)	O(1)#1−V−O(2)	92.70(13)
O(3)−V−O(2)	90.0(2)	O(5)−V−O(2)	88.2(2)

[a] #1: $-x,-y,-z$.

oxygens are almost equal. This shows the absence of mixed valence (V, III) in the dimer. The VOV angle is 105.39°, which shows that the σ-hybridization of bridging oxygen is near sp^3.[12] The σ-hybridization of bridging oxo and hence the bridge angle and V---V separations are subject to major control by the mutual steric requirements of the metal coordination spheres. The principle presented by Parai-Koshits says that when a structure with a center of symmetry is one of several differing very little in energy, it is usually found that the centrosymmetric structure is favored by the crystal packing.[13] The complex anion has a crystallographically imposed center of symmetry, and the molecular symmetry is C_i. Vanadium complexes containing a $[VO(\mu_2\text{-}OR)]_2^{4-}$ ion have five possible cofigurations; they are *anti-orthogonal, anti-coplanar, syn-orthogonal, syn-coplanar, and twist configurations*.[10] Many dinuclear vanadium complexes have been reported for the two orthogonal cofigurations. One example each for anti-coplanar and the twist configuration has also been reported,[10] but a dinuclear complex with a syn-coplanar configuration has not yet been synthesized. From the single-crystal XRD, the present complex is a second example with an anti-coplanar configuration (see Figure 1). Indeed, this is the first example of an ionic vanadyl complex with the anti-coplanar configuration. This complex contains σ and π bonding ligands and is termed class II with equivalent geometries at the vanadium centers.[14] This is supported by the EPR studies; *vide*

(11) Rosenberger, C.; Schrock, R. R.; Davis, W. M. *Inorg. Chem.* **1997**, *36*, 123.

(12) Dean, N. S.; Bond, M. R.; O'Connor, C. J.; Carrano, C. J. *Inorg. Chem.* **1996**, *35*, 7643.

(13) Porai-koshits, M. A. *Zh. Neorg. Khim.* **1968**, *13*, 1233.

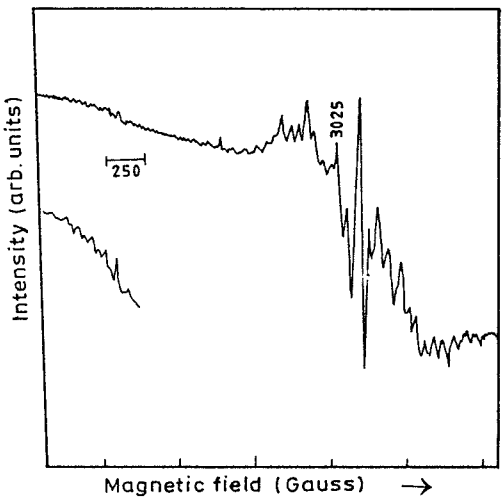

Figure 2. X-band EPR spectrum of frozen aqueous solution at 77 K.

infra. Waters of crystallization are distributed throughout the cell and together with various anionic oxygens make the potassium cations six coordinate. On the basis of the XRD data, theoretical BVS calculations were carried out;[15] the observation of the +4 oxidation state for both vanadiums is consistent with the charge requirements of the molecule.

Electronic Spectra. The band at 564 nm corresponds to a metal d−d transition. The highly intense peak at 303.5 nm corresponds to a ligand transition. The broad and low intensity appearance of absorptions from 600 to 900 nm may be due to metal d−d transitions.

EPR. The EPR spectra of a spin-triplet state are descibed by the spin Hamiltonian[16]

$$H = \beta \bar{B}\mathbf{g}\bar{S} + \bar{S}\mathbf{D}\bar{S} + \bar{I}\mathbf{A}\bar{S} \quad (1)$$

where $\bar{S} = \bar{S}_1 + \bar{S}_2$ is the total spin of the system, $\bar{S}_1$ and $\bar{S}_2$ being the individual spins of the centers 1 and 2, **D**, the zero-field tensor, and **A**, the hyperfine coupling constant tensor. In a coordinate system where **D** is diagonal, one can write

$$H = \beta \bar{B}\mathbf{g}\bar{S} + D[\bar{S}_z^{\,2} - {}^1/_3 S(S+1)] + E(\bar{S}_x^{\,2} - \bar{S}_y^{\,2}) \quad (2)$$

where $D = (2D_{zz} - D_{xx} - D_{yy})/2$ and $E = (D_{xx} - D_{yy})/2$. The D value can be extracted from the half-field transition through the relationship[17]

$$B_{\min}^{\,2} = 1/g^2\beta^2[h^2\nu^2/4 - (D^2 + 3E^2/3)] \quad (3)$$

where B is magnetic field, h is Planck's constant, and ν is the operational frequency.

Solution Spectra. The aqueous frozen solution spectrum of the complex is shown in Figure 2. The spectrum centered at 3200 G consists of the overlapping low- and high-field parallel and perpendicular components each with a 15 line hyperfine structure, with the high- and low-field parallel lines separated by $2D$. The half-field, $\Delta M_s = \pm 2$, transitions are clearly seen at 1600 G with some resolved nuclear hyperfine structure. The spectrum could be simulated satisfactorily with the parameters of $g_\parallel = 1.95$, $g_\perp = 1.98$, $A_\parallel = 83$ G, $A_\perp = 25$ G, and $D = 0.065$ cm^{-1}.

The half-field transitions for the frozen solution spectra at 77 K were very weak with hyperfine structure, and there is uncertainty in finding the $B_{\min}$. The zero-field splitting tensor for exchange-coupled $S = {}^1/_2$ ions contains contributions due to magnetic dipole−dipole and exchange interactions:[18]

$$D = D^{\mathrm{dip}} + D^{\mathrm{ex}} \quad (4)$$

The dipolar part of the zero-field-splitting tensor can be calculated by using the formula of Smith and Pilbrow,[19] which has a very simple form for a centrosymmetrical dimer:

$$D_{\alpha\gamma}^{\ \mathrm{dip}} = {}^1/_2 g_\alpha g_\gamma(\delta_{\alpha\gamma} - 3\sigma_\alpha\sigma_\gamma)\beta^2/r^3 \quad (5)$$

The σ_i variables are the direction cosines between the vector joining the two metal ions and the direction of g_i ($i = x, y, z$); δ_{ij} is Kronecker's δ function. g_z is fixed along the V=O bond direction, g_x is approximately along the O3 bond, and g_y is perpendicular to the g_x and g_z directions. The calculated tensor $\mathbf{D}^{\mathrm{dip}}$ is expressed as follows:

$$\mathbf{D}^{\mathrm{dip}} = \begin{matrix} -0.0010 & -0.0067 & -0.0325 \\ -0.0067 & 0.0216 & -0.0089 \\ -0.0325 & -0.0089 & -0.0201 \end{matrix}$$

Diagonalization yields $D_{xx}^{\mathrm{dip}} = 0.0234$, $D_{yy}^{\mathrm{dip}} = 0.0233$, and $D_{zz}^{\mathrm{dip}} = -0.0463$ cm^{-1}. By using these values, and eq 2, the calculated $D^{\mathrm{dip}} = -0.0696$ and $E^{\mathrm{dip}} = 0$ cm^{-1}. From the simulated frozen solution spectrum the D value is 0.065 cm^{-1}. Since the symmetry of the [V(O)$_2$V] bridge is high, the zero-field-splitting tensor can be treated as axially symmetric. The experimental D value has either the + or − sign. The components of the experimental D value are $D_{xx}^{\mathrm{expt}} = \mp 0.0216$ cm^{-1}, $D_{yy}^{\mathrm{expt}} = \mp 0.0215$ cm^{-1}, and $D_{zz}^{\mathrm{expt}} = \pm 0.0431$ cm^{-1}.

From the D_{ij}^{expt} and theoretically calculated D_{ij}^{dip} values the D_{ij}^{Ex} values are calculated and given as $D_{xx}^{\mathrm{Ex}} = -0.0448$ or -0.0018 cm^{-1}. $D_{yy}^{\mathrm{Ex}} = -0.0449$ or -0.0018 cm^{-1}, and $D_{zz}^{\mathrm{Ex}} = 0.0894$ or 0.0032 cm^{-1} depending up on either of the sign considerations. The exchange part of the zero-field splitting is due to the interaction of the two V^{4+} ground-state wave functions, which are mainly of d_{xy} character. Contributions of the excited states d_{xy}, d_{xz}, and d_{yz} are admixed via LS coupling, however. The components of the corresponding $\mathbf{D}^{\mathrm{ex}}$ tensor can be expressed in terms of the exchanged integrals involved $\boldsymbol{J}_{xy,j}$ ($j = x^2 - y^2$, xz, yz):[18]

$$D_{xx}^{\ \mathrm{ex}} = {}^1/_8(\Delta g_x)^2\boldsymbol{J}_{xy,xz} \quad D_{yy}^{\ \mathrm{ex}} = {}^1/_8(\Delta g_y)^2\boldsymbol{J}_{xy,yz} \quad D_{zz}^{\ \mathrm{ex}} = {}^1/_{32}(\Delta g_z)^2\boldsymbol{J}_{xy,x^2-y^2} \quad (6)$$

$\mathbf{D}^{\mathrm{Ex}}$ is a traceless tensor expressed in terms of a nontraceless tensor $\mathbf{D}^{\mathrm{ex}}$. Here the assumption is $\boldsymbol{J}_{xy,xz}$ and $\boldsymbol{J}_{xy,yz}$ are small with respect to $\boldsymbol{J}_{xy,x^2-y^2}$; i.e., D_{xx}^{ex} and D_{yy}^{ex} must also be small; then

$$D_{zz}^{\ \mathrm{ex}} = {}^1/_{48}(\Delta g_z)^2\boldsymbol{J}_{xy,x^2-y^2} \quad (7)$$

The calculated exchange integral $\boldsymbol{J}_{xy,x^2-y^2}$ is 1569 or 56 cm^{-1}, of which the second value is reasonable. The magnitude of

(14) Schulz, D.; Weyhermuller, T.; Wieghardt, K.; Nuber, B. *Inorg. Chim. Acta* **1995**, *240*, 217.
(15) Thorp, H. H. *Inorg. Chem.* **1992**, *31*, 1585.
(16) Abragam, A.; Bleaney, B. *Electron Paramagnetic Resonance of Transition Ions*; Clarendon Press: Oxford, England, 1970.
(17) Belford, R. L.; Chasteen, N. D.; So, H.; Tapscott, R. E. *J. Am. Chem. Soc.* **1969**, *91*, 4675.
(18) Ozarowski, A.; Reinen, D. *Inorg. Chem.* **1986**, *25*, 1704.
(19) Smith, T. D.; Pilbrow, J. R. *Coord. Chem. Rev.* **1974**, *13*, 173.

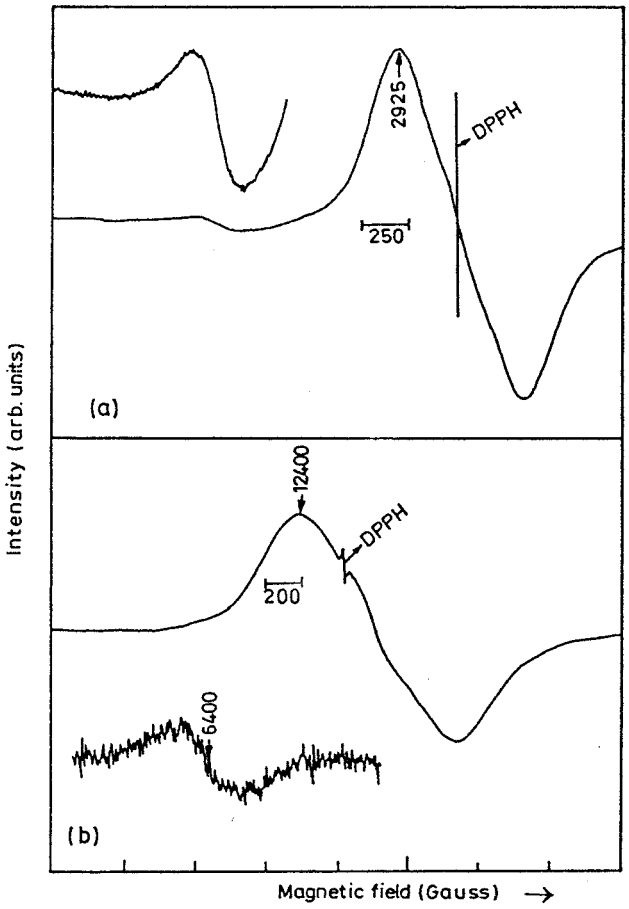

Figure 3. Polycrystalline EPR spectra at 300 K: (a) X-band; (b) Q-band.

exchange integral is small, and hence, the anisotropic exchange interaction cotribution to the zero-field tensor is also not significant. It shows that the interaction between the two metal centers is almost completly dipolar in nature.

Powder Spectra. The X- and Q-band EPR powder spectra of the complex were recorded at room temperature. Figure 3 shows the polycrystalline EPR spectrum at X- and Q-bands. The X-band spectrum shows broad structured bands with no detectable hyperfine structure at $g = 1.9816$. The peak to peak separation was found to be 900 G, with a total spread of 2500 G. The Q-band spectrum shows slightly resolved peaks, and the nature of the peaks is the same as in X-band. From the molecular structure based on XRD and powder EPR at different frequencies, the complex is found to be a ferromagnetically coupled dinuclear metal center. The powder spectra of the neat compound are further subject to intermolecular magnetic interactions, and hence, the fine and hyperfine structures are not resolved. The broad band at half-field from the forbidden $\Delta M_s = \pm 2$ transitions occur at 1650 and 6400 G at X- and Q-band, respectively. The spectral data are consistent with an $S = 1$ spin system that exhibits a small zero-field splitting, as typically observed for other dimeric vanadium(IV) complexes with intramolecular interactions.[10] The 77 K powder EPR spectra recorded at X-band show that there is a slight increase in the signal intensity. As mentioned above, at room temperature, the peaks are not resolved. These observations are indicative of intramolecular ferromagnetic interactions in the exchange-coupled d^1-d^1 systems and thus of a triplet ground state.

The D value can be extracted from eq 3, where $B_{min} = 1650$ G, $\nu = 9.4$ GHz, and $g = 1.9816$; we obtain $D = 0.0640$ cm^{-1} for the X-band powder spectrum at 300 K. This D value is more or less the same as the molecular D value. Due to the bulkiness of the citrate ion, the intermolecular interaction is considerably reduced. The individual zero-field transistions and hyperfine splitting in the powder spectrum are not resolved due to line broadening.

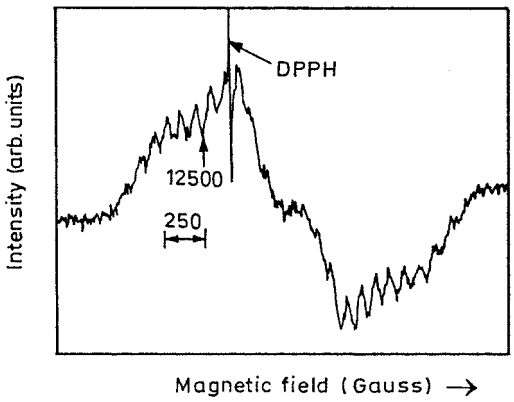

Figure 4. EPR spectrum of the single-crystal orientation at Q-band.

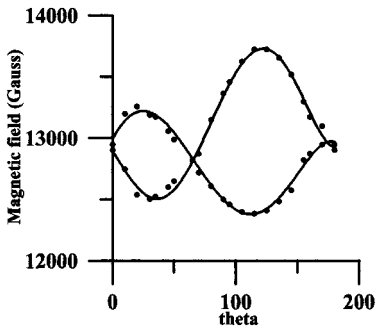

Figure 5. Plot of θ vs magnetic field in the plane of maximum 2D separation.

Attributing D to the magnetic dipolar interaction between the two free electron centers in the complex, we can easily estimate the same from the crystal data. These are as follows: V---V distance = 3.30 Å; angle between V═O bond V---V direction = 37.72°. From the powder EPR $g = 1.9816$ we can calculate the magnitude of this interaction along the V═O bond (θ = 37.72°) or along the V---V direction ($\theta = 0°$). The corresponding values are 0.0207 or 0.0472 cm^{-1}, respectively. The latter one is slightly higher than the experimental value from the powder and single-crystal data (next section). The maximum D_{calcd} will occur at $\theta = 0°$.

Single-Crystal Spectra. Figure 4 shows the X-band spectrum of an oriented single crystal of the complex. Angular variations of the g-values were measured with the magnetic field vector scanning three mutually orthogonal planes at both X- and Q-band frequencies. Figure 5 shows the plot of θ vs magnetic field in Q-band for a plane with maximum separation of 2D. In this plane the plot is identical for both the frequencies. Since $Z = 1$, the EPR spectra also correspond to one magnetically distinct site. In most of the orientations two peaks with hyperfine structure are seen. In single crystals the spectra are due to a single orientation of the molecule and not due to a statistical distribution of orientations. Hence in single-crystal spectra the hyperfine structures are well resolved. In some of the orientations we are able to see the half-field transition. The plot follows the $(1 - 3\cos^2\theta)$ dependence. The maximum separation of 2D is 1360 G. This D value is in agreement with the isolated molecular D value from the frozen solution spectrum.

Variable-Temperature EPR. Variable-temperature polycrystalline EPR spectra were recorded from 20 to 293 K at X-band. Lowering of the temperature does not have much effect on the spectra except for a marginal increase in the intensity. Therefore, in the ground state the vanadium atoms are ferromagnetically coupled.

Generally (μ-OH)$_2$-bridged dinuclear vanadium complexes are antiferromagnetically coupled and a μ-O complex is diamagnetic.[20,21] However, (μ-O)$_2$ complexes are ferromagnetically coupled.[10] A qualitative interpretation of the magnetic interactions in transition metal dimers is usually given by the well-known Goodenough−Kanamori rules, which are based on the interaction between pairs of natural magnetic orbitals.[22] The unpaired electron in oxovanadium(IV) complexes generally resides in a metal-centered orbital with d_{xy} character, with the oxo group oriented along the *z*-axis. For the complex with an anti-coplanar configuration, the orthogonality is certainly dependent on the structural parameters of the [VO(μ_2-O)]$_2$ core, and moreover, the direct overlap between the two magnetic orbitals is expected to be rather small. When V(O)$_2$V is planar and the V---V distance is short, the direct overlap pathway will lead to an antiferomagnetic interaction.[10] For a ferromagnetically coupled system the two magnetic orbitals are orthogonal to each other. In the present complex such a condition favors the observed ferromagnetic interaction. From EPR studies the unpaired electrons are found to be equally interacting with both the nuclei. The mechanism to explain the interaction of the two vanadium centers and the resulting ferromagnetic coupling is due to a "crossed interaction " between singly occupied d_{xy} orbital and empty d_{yz} orbital at either transition metal center using the p_y orbital of a bridging oxygen atom.[10] The $d_{xy}|p_y|d_{yz}$ orbital overlap is depicted in the Figure 6.

In systems where magnetic interactions are less than 0.3 cm^{-1} EPR spectroscopy is a much more sensitive tool than susceptibility measurements, and we get information at the molecular level. In the present system the major interaction is the intramolecular dipole−dipole coupling characterized by a *D* of about 0.065 cm^{-1} with negligible intermolecular magnetic coupling. Temperature-dependent EPR studies clearly show an increased intensity at lower temperatures establishing a ferromagnetic coupling for the ground state of the dimer. The molecules retain their integrity in solution, and the EPR spectra of the frozen solution clearly reveal the chemical equivalence of the two vanadium ions and the through-space dipolar coupling.

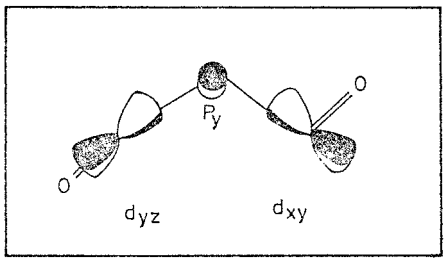

Figure 6. 6. Schematic representation of the "crossed interaction".

ESCA. The ESCA peaks of carbon 1s and potassium 2p overlap with each other. The oxygen 1s peak occurs at 531 eV. The peak at 516 eV corresponds to vanadium $2p_{3/2}$ in the oxidation state of IV.[23] This shows that both the vanadium atoms are in the same oxidation state. There is no indication for mixed valence of the metal centers.

Conclusion

This ionic complex is the first example of an edge-sharing octahedral oxovanadium(IV) dimer that exhibits a ferromagnetic interaction between the metal centers and has an anti-coplanar cofiguration. The magnetic interaction between the two metal center is mainly dipolar in nature. By understanding the magneto−structural correlation of the [VO(μ_2-OR)]$_2^{4-}$ ion by spectroscopic techniques, it is possible to envisage specific magnetic properties of such systems through the choice of ligands employed.

Supporting Information Available: Listings of crystallographic parameters, atomic positional and thermal parameters, anisotropic thermal parameters, and full bond distances and bond angles (10 pages). Ordering information is given on any current masthead page.

IC9707467

(20) Toftlund, H.; Larsen, S.; Murray, K. S. *Inorg. Chem.* **1991**, *30*, 3964.
(21) Wieghardt, K.; Bossek, U.; Volckmar, K.; Swiridoff, W.; Weiss, J. *Inorg. Chem.* **1984**, *23*, 1387.
(22) Ginsberg, A. P. *Inorg. Chim. Acta Rev.* **1971**, *5*, 45.
(23) Ferrer, E. G.; Baran, E. J. *J. Electron Spectrosc. Relat. Phenom.* **1991**, *57*, 189.